

The Existence of Non-unique Steady State Solutions to the RMF Current Drive Equations

W. N. Hugrass

School of Physical Sciences, Flinders University of South Australia,
Bedford Park, S.A. 5042.

Present address: Los Alamos National Laboratory, P.O. Box 1663,
CTR-3, MS/F638, Los Alamos, NM 87545, U.S.A.

Abstract

It is shown that the value of the d.c. current driven in a plasma cylinder by means of a rotating magnetic field (RMF) is not unique for $R/\delta \gtrsim 6$ and $eB_\omega/\nu_{ei}m \approx R/\delta$, where R is the radius of the plasma cylinder, δ is the classical skin depth, ν_{ei} is the electron-ion momentum transfer collision frequency, B_ω is the magnitude of the rotating magnetic field, e is the electron charge and m is the electron mass. This effect is predicted using three distinct approaches: (i) a steady state analysis which ignores the second and higher harmonics of the fields and currents; (ii) a qualitative model which utilizes the analogy between the RMF current drive technique and the operation of the induction motor; (iii) a solution of the initial boundary value equations describing the RMF current drive in cylindrical plasmas.

1. Introduction

The rotating magnetic field (RMF) current drive technique is described in a number of theoretical and experimental papers (see Jones 1984 and the references therein). The purpose of this work is to report an interesting phenomenon that has not been recognized in earlier papers, namely that the value of the steady state d.c. current driven in a given plasma cylinder is not unique for $R/\delta \gtrsim 6$ and $eB_\omega/\nu_{ei}m \approx R/\delta$, where R is the radius of the plasma cylinder, δ is the classical skin depth, ν_{ei} is the electron-ion momentum transfer collision frequency, B_ω is the magnitude of the rotating magnetic field, e is the electron charge and m is the electron mass. This effect is more pronounced for large values of R/δ ; the findings of this work may, therefore, be useful in the design of future experiments (which will have larger values of R/δ).

In Section 2 we present the simplest model that can be adopted to study the RMF current drive: an infinitely long plasma cylinder with a massless cold electron fluid and a uniform distribution of immobile ions. An approximate steady state analysis of this model is given in Section 3. In this steady state analysis, the effects of the second and higher harmonics of the fields and currents are neglected. The approximate equations are much simpler than the general equations and the simplicity of the analysis allows one to obtain a deeper insight into the physical mechanism of the RMF current drive. It is also possible to obtain solutions for large values of R/δ in a reasonable amount of computing time. The solutions presented in Section 3 reveal the fact that the value of the d.c. current driven in the plasma is not unique for $R/\delta \gtrsim 6$ and $\omega_{ce}/\nu_{ei} (= eB_\omega/\nu_{ei}m) \approx R/\delta$.

The analogy between the RMF current drive technique and the operation of the induction motor (Hugrass 1984) is briefly reviewed in Section 4. Here it is shown that the predictions of an analysis which examines the operation of a simple induction motor are in agreement with the results presented in Section 3.

The analysis presented in Sections 3 and 4 indicates the existence of three different steady state solutions for a certain range of ω_{ce}/v_{ei} . Only two of these are stable solutions which can be obtained using an initial value analysis. This conclusion is confirmed in Section 5 where the initial boundary value equations are solved for R/δ values of 4 and 7. It is found that, for $R/\delta = 7$ and in the region $\omega_{ce}/v_{ei} \gtrsim 7$, the steady state value of the d.c. driven current depends on whether the RMF approaches its final steady state value from a higher or a lower initial value.

The results and conclusions are given in Section 6 where the relevance of this effect to the interpretation of some early experimental results and to the design of future experiments is discussed. The limitations of the analysis are also identified.

2. Physical Model

For the purpose of the analysis presented in Sections 3 and 5 we consider the simplest physical model of the RMF current drive (Jones and Hugrass 1981; Hugrass and Grimm 1981). In this model the infinitely long cylindrical plasma is composed of a massless cold electron fluid and a uniform immobile ion population. The resistivity η is uniform and isotropic and is related to the number density n and the electron-ion momentum transfer collision frequency ν_{ei} through the classical formula

$$\eta = m\nu_{ei}/ne^2. \quad (1)$$

The externally applied magnetic field is given by

$$\mathbf{B} = B_\omega \cos(\omega t - \theta) \hat{\mathbf{r}} + B_\omega \sin(\omega t - \theta) \hat{\boldsymbol{\theta}} + B_a \hat{\mathbf{z}}, \quad (2)$$

where B_a is a uniform axial magnetic field. The fields and currents satisfy Maxwell's equations

$$\nabla \times \mathbf{E} = -\partial \mathbf{B} / \partial t, \quad \nabla \times \mathbf{B} = \mu_0 \mathbf{J} \quad (3, 4)$$

and the appropriate form of the generalized Ohm law (see Jones and Hugrass 1981)

$$\mathbf{E} - (1/ne) \mathbf{J} \times \mathbf{B} = \eta \mathbf{J}. \quad (5)$$

3. Steady State Analysis

In this section, we develop an approximate steady state analysis for the model described in Section 2. It has been shown that, in the steady state, all the physical quantities (i.e. scalar quantities or components of vector quantities in cylindrical coordinates) are functions of $\omega t - \theta$ (Hugrass 1982). It follows that any such quantity Q can be represented as a sum of harmonics:

$$Q(r, \theta, t) = Q_0(r) + \sum_m Q_m(r) \exp\{i m(\omega t - \theta)\}.$$

It has also been shown that each physical quantity can have either even harmonics (including a d.c. part) or odd harmonics. For the given applied fields, the field and

current components which have a d.c. part and even harmonics are $B_z, E_\theta, E_r, J_\theta$ and J_r . The field and current components which have only odd harmonics are B_r, B_θ, E_z and J_z . In the following analysis, the second and higher harmonics will be neglected. The equations will relate either steady components or the complex amplitudes of first harmonic components. The steady components are denoted by symbols with the subscript zero, e.g. $E_{\theta 0}, J_{\theta 0}, \dots$ etc., while the first harmonic parts are denoted by the subscript one, e.g. E_{z1}, J_{z1}, \dots etc. The standard phasor notation is followed, for example,

$$E_z = \text{Rel}[E_{z1} \exp\{i(\omega t - \theta)\}].$$

Using Faraday's law (3) one obtains

$$E_{\theta 0} = 0, \quad E_{z1} = \omega r B_{r1}. \tag{6, 7}$$

The θ and z components of Ohm's law (5) are

$$E_{\theta 0} - (1/2ne)\text{Rel}[J_{z1} B_{r1}^*] = \eta J_{\theta 0}, \tag{8}$$

$$E_{z1} + (1/ne)J_{\theta 0} B_{r1} = \eta J_{z1}, \tag{9}$$

where the asterisk denotes the complex conjugate. Using equations (7) and (9) we conclude that E_{z1} and J_{z1} are in phase. It follows that

$$J_{\theta 0} = -(1/2\eta ne)J_{z1} B_{r1}^*, \tag{10}$$

$$J_{z1} = \frac{1}{\eta} \frac{E_{z1}}{1 + \frac{1}{2}B_{r1} B_{r1}^*/(ne\eta)^2}. \tag{11}$$

The other equation relating J_{z1} to E_{z1} is obtained by using Maxwell's equations (3) and (4):

$$\nabla^2 E_{z1} = i\omega\mu_0 J_{z1}. \tag{12}$$

It follows that

$$\nabla^2 E_{z1} - \frac{i\omega\mu_0/\eta}{1 + \frac{1}{2}E_{z1} E_{z1}^*/(ne\omega\eta)^2} E_{z1} = 0 \quad \text{for } 0 \leq r \leq R, \tag{13a}$$

$$\nabla^2 E_{z1} = 0 \quad \text{for } r \geq R. \tag{13b}$$

The solution to equation (13b) which matches the externally applied field (2) for $r \gg R$ is given by

$$E_{z1} = \omega r B_\omega + C_1(R/r)\omega R B_\omega, \tag{14}$$

where C_1 is an arbitrary constant. The value of C_1 is obtained by invoking the continuity of B_{r1} and $B_{\theta 1}$ at the boundary surface $r = R$; it follows that both E_{z1} and $\partial E_{z1}/\partial r$ are continuous at $r = R$. The solution to (13a) in the region $0 \leq r \leq R$ should, therefore, satisfy the boundary condition

$$E_{z1} + R \partial E_{z1}/\partial r|_{r=R} = 2\omega R B_\omega. \tag{15}$$

The analysis is made more transparent by normalizing equations (13a) and (15). We define the dimensionless quantities:

$$E = E_{z1}/\omega RB_\omega, \quad \lambda^2 = R^2/\delta^2 = (\mu_0 \omega/2\eta)R^2, \quad (16a, b)$$

$$\gamma_\omega = \omega_{ce}/v_{ei} = eB_\omega/mv_{ei} = B_\omega/n\eta, \quad (16c)$$

$$\gamma^2(r) = B_{r1} B_{r1}^*/(n\eta)^2, \quad X = r/R. \quad (16d, e)$$

The normalized axial electric field satisfies the equation

$$\frac{d^2 E}{dX^2} + \frac{1}{X} \frac{dE}{dX} - \left(\frac{1}{X^2} + \frac{2i\lambda^2}{1 + \frac{1}{2}\gamma_\omega^2 EE^*/X^2} \right) E = 0 \quad (17)$$

in the region $0 \leq X \leq 1$, and

$$E + dE/dX = 2 \quad (18)$$

at $X = 1$. The field and current components can be obtained in terms of E :

$$E_{z1} = \omega RB_\omega E, \quad (19a)$$

$$B_{r1} = (R/r)B_\omega E = B_\omega E/X, \quad (19b)$$

$$\begin{aligned} J_{z1} &= \frac{1}{1 + \frac{1}{2}e^2 B_{r1} B_{r1}^*/m^2 v_{ei}^2} \frac{\omega RB_\omega E}{\eta} \\ &= \frac{1}{1 + \frac{1}{2}\gamma^2(r)} \frac{E_{z1}}{\eta}, \end{aligned} \quad (19c)$$

$$\begin{aligned} J_{\theta 0} &= -\frac{\frac{1}{2}e^2 B_{r1} B_{r1}^*/m^2 v_{ei}^2}{1 + \frac{1}{2}e^2 B_{r1} B_{r1}^*/m^2 v_{ei}^2} n\omega r \\ &= -\frac{1}{1 + 2/\gamma^2(r)} n\omega r. \end{aligned} \quad (19d)$$

It is clear from equation (17) that the system is completely specified in terms of two dimensionless parameters. These are the ratio of the plasma radius R to the classical skin depth δ , $\lambda = R/\delta$, and the ratio of the electron cyclotron frequency ω_{ce} to the electron-ion momentum transfer collision frequency v_{ei} , $\gamma_\omega = eB_\omega/mv_{ei} = \omega_{ce}/v_{ei}$. It is not possible to obtain a general analytical solution to equation (17) for arbitrary values of λ and γ_ω . However, we will consider here two limiting cases where equation (17) is approximately linear and an analytical solution can be obtained.

Linear limit $\gamma_\omega \rightarrow 0$. In this limit, equation (17) is simplified to

$$\frac{d^2 E}{dX^2} + \frac{1}{X} \frac{dE}{dX} - \left(\frac{1}{X^2} + 2i\lambda^2 \right) E = 0. \quad (20)$$

The solution that satisfies the boundary condition (18) is

$$E = \frac{2}{(1+i)\lambda I_0((1+i)\lambda)} I_1((1+i)\lambda X). \quad (21)$$

In this linear limit, the field and current components are given by

$$E_{z1} = \frac{2\omega RB_\omega}{(1+i)\lambda I_0((1+i)\lambda)} I_1((1+i)\lambda X), \quad (22a)$$

$$r_1 B = \frac{B_\omega}{I_0((1+i)\lambda)} \frac{2I_1((1+i)\lambda X)}{(1+i)\lambda X}, \quad (22b)$$

$$J_{z1} = E_{z1}/\eta, \quad J_{\theta 0} = 0. \quad (22c, d)$$

Fig. 1 shows b_θ and b_r (i.e. $|B_{\theta 1}|/B_\omega$ and $|B_{r1}|/B_\omega$) plotted against r/R for λ values of 4 and 7, which illustrates the classical skin effect.

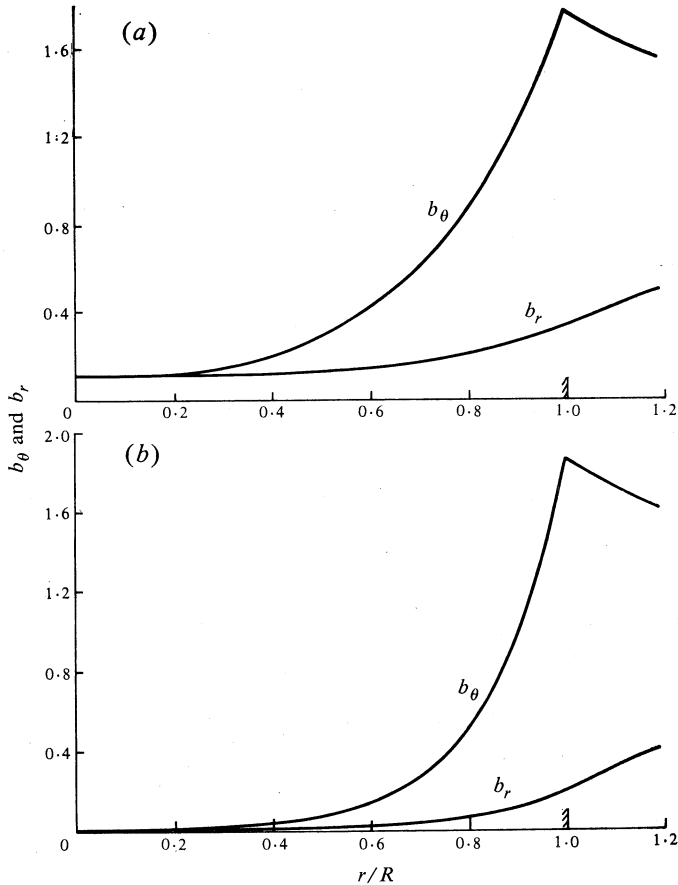


Fig. 1. Normalized azimuthal and radial components of the magnetic field plotted against r/R for λ values of (a) 4 and (b) 7.

Strongly nonlinear limit $\gamma_\omega \gg \lambda$. In the limit $\gamma_\omega \gg \lambda$ the system is strongly nonlinear since the (nonlinear) Hall term in Ohm's law (5) is much larger than the (linear) resistive term. It is surprising that equation (17) becomes linear in this limit:

$$\frac{d^2 E}{dX^2} + \frac{1}{X} \frac{dE}{dX} - \frac{1}{X^2} E = 0. \quad (23)$$

The solution to this equation is

$$E = X \tag{24}$$

and the field and current components are given by

$$E_{z1} = \omega R B_\omega E = \omega r B_\omega, \quad B_{r1} = B_\omega, \tag{25a, b}$$

$$J_{z1} = 0, \quad J_{\theta 0} = -n\omega r. \tag{25c, d}$$

This solution corresponds to a perfect penetration of the RMF into the plasma (equation 25b) and to the electron fluid rotating synchronously with the magnetic field (equation 25d).

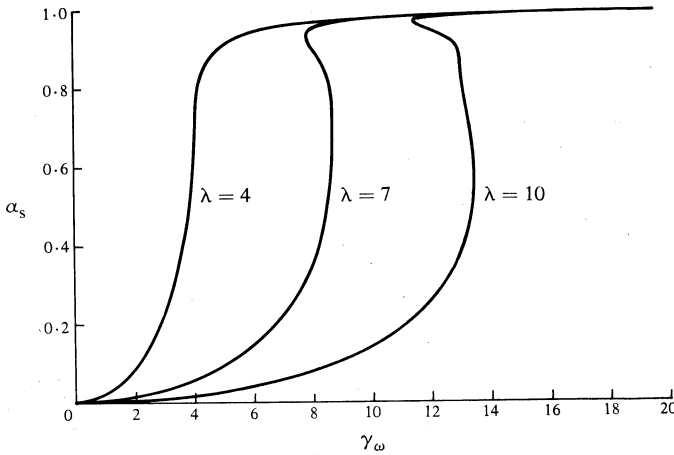


Fig. 2. Normalized steady azimuthal current α_s plotted against γ_ω for the three values of λ indicated.

It is thus seen that analytical solutions to equation (17) can be obtained for $\gamma_\omega \ll 1$ and for $\gamma_\omega \gg \lambda$. In the intermediate region, where $1 \leq \gamma_\omega \leq \lambda$, the solution is obtained numerically. The numerical method for solving equation (17) for general γ_ω and λ is described in the Appendix. Fig. 2 shows the variation of the normalized steady azimuthal current α_s with γ_ω for different values of λ . Here $\alpha_s = I_{\theta 0}/I_{\theta 0}^M$, where the total azimuthal current per unit length is

$$I_{\theta 0} = \int_0^R J_{\theta r} dr,$$

and

$$I_{\theta 0}^M = \int_0^R n\omega r dr = \frac{1}{2}n\omega R^2.$$

It is seen that for $\gamma_\omega \ll \lambda$, α_s is much smaller than 1, while for $\gamma_\omega \gg \lambda$, α_s is very nearly equal to its maximum possible value of 1. In the region $\gamma_\omega \sim \lambda$, α_s is a very sensitive function of γ_ω . It is also seen that for $\lambda \gtrsim 6$ the curve has a region of negative slopes. In this region, α_s can have one of three possible values for the same γ_ω . This mean.

that it is possible to drive three different values of the steady state d.c. azimuthal current in a given plasma cylinder for the same value of the applied RMF. The three possible steady states are characterized by different degrees of the penetration of the RMF in the plasma. Fig. 3 shows b_r plotted against r/R for $R/\delta = 10$ and $\omega_{ce}/\nu_{ei} = 12$ and for the three steady states α_s of 0.26, 0.83 and 0.85. It is clear that the higher values of α_s correspond to steady states with deeper penetration of the RMF in the plasma.

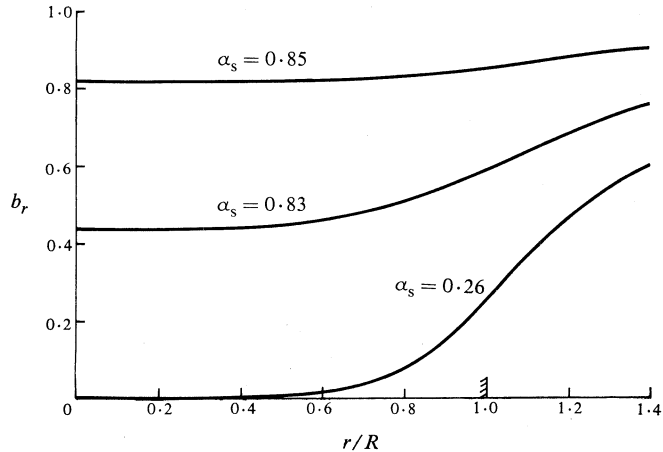


Fig. 3. Plot of b_r against r/R for $R/\delta = 10$ and $\omega_{ce}/\nu_{ei} = 12$. The three curves correspond to the three possible values of α_s indicated.

4. Induction Motor Model

In the RMF current drive technique, the RMF continually imparts angular momentum to the electron fluid. The electron fluid rotates under the influence of this electromagnetic torque and, in the steady state, the electromagnetic torque is exactly balanced by a retarding frictional (collisional) torque due to the relative rotation between the electron fluid and the ion fluid. The ion fluid is essentially stationary and relaxes the angular momentum, which is imparted to it collisionally (from the electron fluid), to the surrounding environment.

In a previous paper (Hugrass 1984) it has been shown that the RMF current drive technique is analogous to the operation of the induction motor. In both systems, the medium for the transfer of power and angular momentum is an RMF generated by means of a polyphase winding. The electron fluid is analogous to the rotor and the ion fluid to the mechanical load. The analogy, although qualitative in nature, proved useful in understanding the physics of the RMF current drive. It will be shown now that this simple model confirms the findings obtained by the steady state analysis in Section 3.

Fig. 4 shows a conceptual induction motor. The magnetic field, which has a magnitude B_ω and rotates about the axis at an angular frequency ω , is generated by means of a polyphase stator winding (not shown). The rotor consists of a rectangular coil of resistance R_c and inductance L_c . In the steady state the rotor rotates at an angular frequency $\omega_m \leq \omega$ and the electromagnetic torque T is exactly equal to the

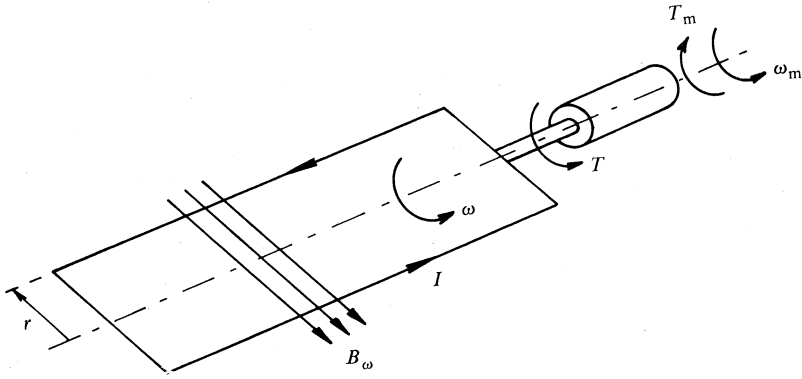


Fig. 4. A conceptual induction motor.

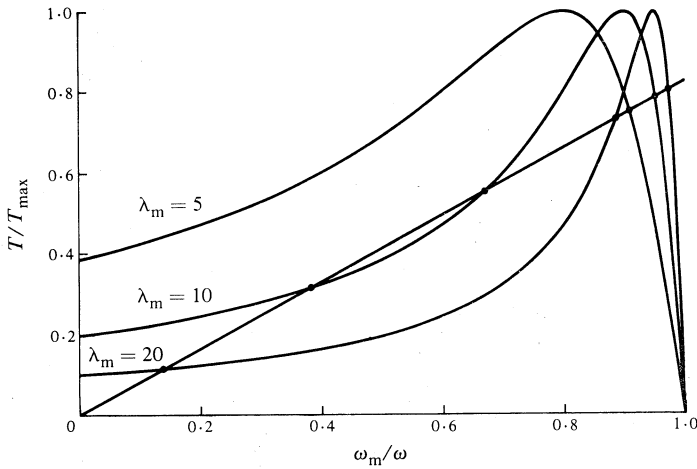


Fig. 5. Normalized torque T/T_{max} plotted against normalized angular frequency ω_m/ω for the three values of λ_m indicated. The load line corresponds to a mechanical load torque proportional to the angular frequency.

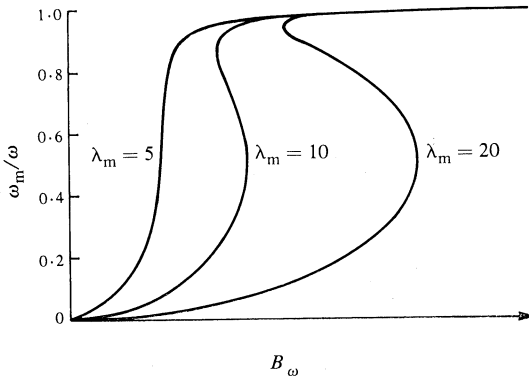


Fig. 6. Plot of ω_m/ω against B_ω for an induction motor for the three values of λ_m indicated.

retarding torque of the mechanical load T_m . The performance of the motor depends on the value of the dimensionless parameter $\lambda_m = \omega L_c / R_c$. This parameter is analogous to the parameter $\lambda = R/\delta$ defined in Section 3 for the RMF current drive. Fig. 5 shows the normalized torque T/T_{max} plotted against the normalized angular frequency ω_m/ω for λ_m values of 5, 10 and 20. A load line is also shown, corresponding to T proportional to ω_m . The operating point is defined by the intersection of the load line and the motor characteristics since it must satisfy both. It is seen that there is a unique operating point for $\lambda_m = 5$. For λ_m values of 10 and 20, there are three possible operating points. As explained in Hugrass (1984), the curves of ω_m/ω against B_ω for the induction motor are analogous to the curves of I/I_θ^M against ω_{ce}/v_{ei} for the RMF current drive system. Fig. 6 shows these curves for λ_m values of 5, 10 and 20. These curves correspond to RMF current drive systems with different R/δ (one should again stress the qualitative nature of this argument). It is seen that the value of the driven current is not unique for systems with large R/δ , in complete qualitative agreement with the results obtained in Section 3.

5. Initial Value Problem

In this section we study the physical model presented in Section 2 as a mixed initial boundary value problem. It has been shown (Jones and Hugrass 1981; Hugrass and Grimm 1981) that all the field and current components can be expressed in terms of the axial component of the vector potential A_z and the axial component of the magnetic field B_z (with A defined by $B = \nabla \times A$). These two components satisfy the equations

$$\frac{\partial A_z}{\partial t} = \frac{\eta}{\mu_0} \nabla^2 A_z + \frac{1}{\mu_0 n e r} \left(\frac{\partial A_z}{\partial r} \frac{\partial B_z}{\partial \theta} - \frac{\partial A_z}{\partial \theta} \frac{\partial B_z}{\partial r} \right), \tag{26}$$

$$\frac{\partial B_z}{\partial t} = \frac{\eta}{\mu_0} \nabla^2 B_z + \frac{1}{\mu_0 n e r} \left(\frac{\partial \nabla^2 A_z}{\partial r} \frac{\partial A_z}{\partial \theta} - \frac{\partial \nabla^2 A_z}{\partial \theta} \frac{\partial A_z}{\partial r} \right). \tag{27}$$

The physical significance of equations (26) and (27) becomes more apparent if they are written in a dimensionless form. This transformation is defined by the equations

$$T = \omega t, \quad X = r/R, \quad \nabla'^2 = R^2 \nabla^2, \tag{28a, b, c}$$

$$A = e A_z / v_{ei} m R = \gamma_\omega A_z / R B_\omega, \quad B = 2 B_z / \mu_0 n e \omega R^2. \tag{28d, e}$$

The dimensionless equations are

$$\frac{\partial A}{\partial T} = \frac{1}{2\lambda^2} \nabla'^2 A + \frac{1}{2X} \left(\frac{\partial A}{\partial X} \frac{\partial B}{\partial \theta} - \frac{\partial A}{\partial \theta} \frac{\partial B}{\partial X} \right), \tag{29}$$

$$\frac{\partial B}{\partial T} = \frac{1}{2\lambda^2} \nabla'^2 B + \frac{1}{2\lambda^4 X^2} \left(\frac{\partial \nabla'^2 A}{\partial X} \frac{\partial B}{\partial \theta} - \frac{\partial \nabla'^2 A}{\partial \theta} \frac{\partial B}{\partial X} \right). \tag{30}$$

The boundary condition for A is given in terms of its harmonics ($A_m, m = 1, 2, \dots$) defined by

$$A = \sum_m A_m \exp(i m \theta). \tag{31}$$

Each harmonic satisfies the condition

$$A_m(1) + \partial A_m / \partial X |_{X=1} = 2A_{m \text{ ex}}, \tag{32}$$

where

$$A_{1 \text{ ex}} = \gamma_\omega(t), \tag{33}$$

$$A_{m \text{ ex}} = 0, \quad \text{for } m \neq 1. \tag{34}$$

The boundary condition for B is

$$B(1) = 2B_a / \mu_0 n e \omega R^2, \tag{35}$$

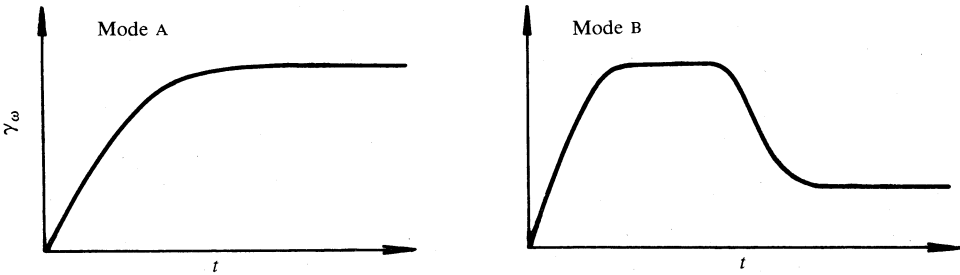


Fig. 7. Modes of time variation of the parameter γ_ω .

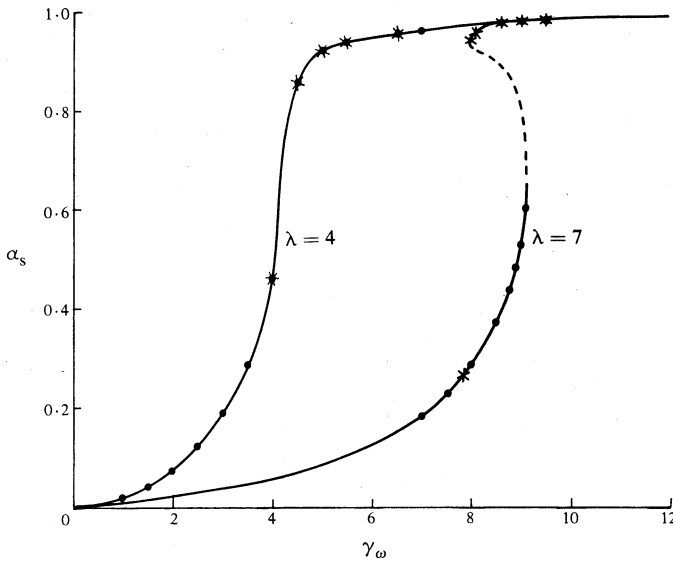


Fig. 8. Plot of α_s against γ_ω for λ values of 4 and 7.

where B_a is the value of the externally applied steady axial field. We note that the value of B_a merely introduces an additive constant since only derivatives of B appear in equations (29) and (30).

It is clear from equations (29), (30) and (33) that the system is completely defined in terms of two dimensionless parameters, namely $\lambda = R/\delta$ and $\gamma_\omega = eB_\omega/mv_{ej}$. The equations are solved numerically using the finite difference method for a certain value

of λ . (Details of the numerical method are given in Hugrass and Grimm 1981.) The value of the parameter α_s ($= I_{\theta 0}/I_{\theta 0}^M$ in the steady state) is obtained from the solution using the equation

$$\alpha_s = |B(X=0) - B(X=1)|. \quad (36)$$

The parameter γ_ω varies with time in either one of the two modes depicted schematically in Fig. 7. For mode A, $\gamma_\omega(t)$ grows monotonically from the initial value, $\gamma_\omega(0) = 0$, to its steady state value. For mode B, $\gamma_\omega(t)$ grows initially to a high transient value then decays exponentially to a smaller steady state value. Fig. 8 shows α_s plotted against γ_ω for λ values of 4 and 7. Points obtained by using the $\gamma_\omega(t)$ variation as in mode A are denoted by circles, whereas points obtained with the $\gamma_\omega(t)$ variation in mode B are denoted by stars. It is seen that, for $\lambda = 4$, α_s does not depend on the mode of variation of $\gamma_\omega(t)$ but only on the steady state value γ_ω , and the curve is single valued. For $\lambda = 7$, the curve is not single valued in the region $\gamma_\omega \gtrsim 7$. It is seen that the value of α_s obtained with $\gamma_\omega(t)$ varying as in mode B is larger than that obtained for $\gamma_\omega(t)$ in mode A (see Fig. 7). The dotted part of the curve in Fig. 8 corresponds to a third value of α_s which is not accessible using the initial boundary value approach. This part of the curve can only be obtained by using a steady state analysis as in Sections 3 and 4. It is worth while to mention here that this multi-valued nature of the characteristic curve of α_s against γ_ω was not recognized in the earlier work of Hugrass and Grimm (1981) since $\gamma_\omega(t)$ was allowed to vary only as in mode A. As mentioned in Section 3, the non-uniqueness of the solution becomes more apparent for higher values of λ . Unfortunately the computing time increases very rapidly with λ and the value of 7 was chosen as a compromise.

We also note that, although the results obtained in this section are qualitatively similar to those obtained in Section 3, there is a noticeable quantitative difference in the value of α_s at the transition region where α_s is very sensitive to γ_ω . This difference is attributed to the neglect of the second and higher harmonics in the analysis in Section 3.

6. Discussion and Conclusions

In this paper we report a new property of RMF current drive systems, namely that the steady state value of the d.c. current driven in a given plasma cylinder is not unique for $R/\delta \gtrsim 6$ and $\omega_{ce}/v_{ei} \sim R/\delta$. We note that future experiments will have larger dimensions and possibly higher electron temperatures, and consequently the value of R/δ is expected to be very high. As stated in Section 3, the non-uniqueness of the solution becomes more apparent the higher the value of R/δ . Guided by the results of this work, it may be advisable to design r.f. power sources capable of delivering high power for a short period followed by a lower power for a much longer period, i.e. the r.f. power varies in time as for mode B in Fig. 7. It may be possible to obtain steady state configurations which are not accessible if the r.f. power rises monotonically to the steady state value. There is already some experimental evidence supporting this conclusion (Kühnapfel and Tucek 1983). In this experiment, it was observed that the rotating field did not penetrate into the plasma unless its amplitude exceeded a certain threshold value. But once it penetrated, it continued to do so even though its magnitude was reduced to about one-tenth of the threshold value.

It must be admitted, however, that these results can be explained by a number of alternative arguments. For example, it is possible that the plasma temperature increases during the early phase of the discharge and hence the value of the threshold decreases. Unfortunately, there are not sufficient measurements to arrive at a definite conclusion. It is also recognized that the results were obtained by using very simplified models which are significantly different from the experimental situation. The models assume infinitely long plasma cylinders, whereas most of the experiments are carried out on compact toroidal plasmas. The interactions between the plasma and r.f. circuit, the energy and particle transport, and the motion of the ion fluid were not treated. These will be the subject of future work.

Acknowledgments

The author acknowledges many fruitful discussions with Professor I. R. Jones. This work was supported by N.E.R.D.D.C.

References

- Hugrass, W. N. (1982). *J. Plasma Phys.* **28**, 369.
 Hugrass, W. N. (1984). *Aust. J. Phys.* **37**, 509.
 Hugrass, W. N., and Grimm, R. C. (1981). *J. Plasma Phys.* **26**, 455.
 Jones, I. R. (1984). The rotating magnetic field technique of driving current and its application in the Rotamak. Flinders Univ. Rep. No. FUPH-R-189.
 Jones, I. R., and Hugrass, W. N. (1981). *J. Plasma Phys.* **26**, 441.
 Kühnapfel, M., and Tuczek, H. (1983). Proc. IAEA Tech. Comm. Meeting on Non-inductive Current Drive in Tokamaks, Culham, Vol. 2, p. 417 (UKAEA: Abingdon).

Appendix. Numerical Solution to the Steady State Equation

It is shown in Section 3 that the normalized electric field $E = E_{z1}/\omega RB_\omega$ satisfies the equation

$$\frac{d^2E}{dX^2} + \frac{1}{X} \frac{dE}{dX} - \left(\frac{1}{X^2} + \frac{2i\lambda}{1 + \frac{1}{2}\gamma_0^2 EE^*/X^2} \right) E = 0, \quad (\text{A1})$$

for $0 \leq X \leq 1$, together with the boundary condition

$$E + dE/dX = 2 \quad (\text{A2})$$

at the boundary surface $X = 1$. This is a one-dimensional nonlinear boundary value problem. Using a finite difference approximation, the problem can be reduced to a system of coupled nonlinear algebraic equations. In order to avoid the difficulty involved in solving such a system of nonlinear equations, we have obtained the solution for the equivalent equations governing the normalized field

$$Y = \frac{E_{z1}}{\omega RB_{r1}(0)} = \frac{B_\omega}{B_{r1}(0)} E. \quad (\text{A3})$$

This normalized field satisfies the equations

$$\frac{d^2Y}{dX^2} + \frac{1}{X} \frac{dY}{dX} - \left(\frac{1}{X^2} + \frac{2i\lambda^2}{1 + \gamma_0^2 YY^*/X^2} \right) Y = 0 \quad (\text{A4})$$

for $0 \leq X \leq 1$ and

$$Y + dY/dX = 2\gamma_\omega/\gamma_0 \quad (\text{A5})$$

at $X = 1$, where

$$\gamma_0 = eB_{r1}(0)/v_{ei}m. \quad (\text{A6})$$

The field Y satisfies the conditions

$$dY/dX = 1, \quad d^2Y/dX^2 = 0 \quad (\text{A7, A8})$$

at $X = 1$.

For given values of λ and γ_0 , one can solve equation (A5) together with the initial condition (A7) as an initial value problem. [We note that the extra condition given in (A8) is needed since the equation is singular at $r = 0$.] The value of γ_ω corresponding to this solution is then evaluated using equation (A5). Thus, the set of solutions for a certain value of λ and a range of values of γ_ω is obtained by solving the initial value problem for this value of λ over the corresponding range of γ_0 . (The relationship between γ_0 and γ_ω is not known *a priori*.)

